

Dynamical Transition in Quasistatic Fluid Invasion in Porous Media

Marek Cieplak^(a) and Mark O. Robbins

Department of Physics and Astronomy, Johns Hopkins University, Baltimore, Maryland 21218

(Received 1 February 1988)

Numerical simulations of capillary displacement in 2D porous media indicate a dynamical critical transition as the contact angle θ of the invading fluid varies. In the nonwetting limit ($\theta=180^\circ$), growth patterns are fractal as in the invasion percolation model. As θ decreases, cooperative smoothing mechanisms involving neighboring throats become important. The typical width of invading fingers appears to diverge at a critical angle which depends on porosity. Below this angle the fluid floods the system uniformly.

PACS numbers: 68.10.Gw, 47.55.Mh, 68.10.Cr

Many recent papers have addressed fluid invasion into a porous medium filled with an immiscible fluid.¹⁻⁵ Such systems are ideal models for studies of pattern formation in growth and are of great practical interest. As the velocity, viscosity, and pore geometry are varied, the pattern formed by the invading fluid changes from compact to dendritic¹ or to a fractal of either a percolation^{2,3} or diffusion-limited aggregation^{4,5} type. The wetting properties of the fluids also play a crucial role in pattern selection,^{6,7} but their influence has received less theoretical attention.

In this paper, we study fluid invasion in the quasistatic limit where capillary forces dominate viscous ones. Microscopic pore-level simulations of interface evolution are described for model 2D porous media as a function of the contact angle θ of the invading fluid (Fig. 1).⁸ When the invading fluid is nonwetting (NW), $\theta=180^\circ$, the interface is similar to the fractal produced by the invasion percolation (IP) model.^{2,3} The mean width of an invading finger, \bar{w} , is of order the pore size. As θ decreases, \bar{w} appears to diverge at a critical angle θ_c . Below θ_c the fluid floods the medium in a compact pattern. This smoothing of the fluid interface results from cooperative invasion by neighboring pores and is absent

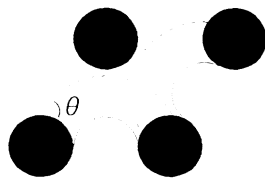


FIG. 1. Four equal-radius disks ($r=0.25$) and connecting arcs at the bursting pressure for $\theta=180^\circ$ (solid lines) and $\theta=60^\circ$ (dashed lines). The invading fluid is below the interface and θ is measured as indicated. All arcs would burst to the disk at the upper left. For $\theta=60^\circ$ overlap occurs first and the new interface connects the lower-left and upper-right disks. This arc would touch the upper-left disk leading to further growth. If the disk in the upper left were larger it might be touched before overlap occurred and would become part of the interface.

in the IP model which predicts a fractal pattern with pore-scale structure for all θ .

Experimental evidence for interface smoothing as the invading fluid becomes more wetting is well established in etched networks of tubes⁶ and thin Hele-Shaw cells packed with glass beads.⁷ When viscous and boundary effects become negligible and θ is near 180° (NW) the pattern is an IP fractal with pore-scale fingers. For invasion by a wetting (W) fluid, the interface is nearly flat. Even at high velocities, viscous fingers in the W case remain much larger than the pore size.⁷ There appears to be a strong smoothing force analogous to a surface tension at long length scales. Similar behavior is observed in porous rocks.⁹ Note that since it is hard to vary θ continuously, only the limiting behavior is known in these systems.

To model the nearly 2D flow observed in Ref. 7, we use a 2D array of disks with random radii. This should be similar to a cross section through a random bead pack and allows a full solution for the interface shape. For simplicity we place the disks on an $L \times L$ triangular or square lattice with unit spacing, and L between 300 and 800. Radii are uniformly distributed within an interval $[r_1, r_2]$. The parameters describing the systems studied are given in Table I. Similar results were obtained when the disk centers were randomly shifted from lattice sites.

At a fixed pressure difference, p , a stable interface consists of a set of arcs between consecutive disks. Each arc must have radius $r = \gamma/p$, where γ is the surface tension. It must also attach to both disks at the proper θ (Fig. 1).⁸ To minimize boundary effects, our growth

TABLE I. Systems studied and observed critical angles.

System	r_1	r_2	ϕ	θ_c (deg)
Triangular A	0.05	0.48	0.665	50
Triangular B	0.22	0.32	0.730	69
Triangular C	0.38	0.48	0.322	29
Square D	0.05	0.48	0.709	58

simulations start from a ring connecting six or more disks near the center of the lattice. For any starting ring and θ the interface is stable over a range of p . However, as p increases a section of the interface becomes unstable and flow starts.

In principle flow should be simulated by our solving for the viscous pressure drop in the medium, and integrating the velocity for each section of the interface. However, in the quasistatic limit and at constant p , the interface moves rapidly between nearly stable configurations of the interface. One may model the dynamics as a stepwise process where each unstable section of the interface moves to the next stable or nearly stable configuration in turn.

There are three basic types of instability and corresponding growth mechanism (Fig. 1):

(1) "Burst"—there is no stable arc connecting two disks at p . The interface jumps forward to connect to the nearest disk.

(2) "Touch"—the arc connecting two disks intersects another disk at the wrong θ . The interface must connect to this intermediate disk.

(3) "Overlap"—nearby arcs overlap. The disk to which both arcs connect is removed from the interface.

Figure 1 shows the interfaces between three disks at the bursting pressures for $\theta=179^\circ$ and 60° . Note that in the NW case the arcs lie in the narrowest part of the throats. Both arcs would burst to the fourth disk which is not yet on the interface. As θ decreases, the arcs spread into the pore space and touches and overlaps become more likely. For $\theta=60^\circ$ and the configuration shown in Fig. 1, overlap occurs at a lower p than bursts or touches. In fact, even arcs between three collinear disks overlap below the pressure for bursts. The variation in importance of the growth mechanisms with θ leads to dramatic changes in pattern.

Growth is determined by fixing p and finding the unstable arcs. These are advanced sequentially along the interface to simulate uniform growth. Arcs unstable against bursts are represented by stable arcs of minimal radius (highest p) in tests for touches and overlaps. Bursts occur to the disks which are closest to such arcs and in the angle subtended by them. If more than one type of instability occurs for a given arc, touches are eliminated first and bursts last—touches and overlaps imply an excessive advance.

Advancement of an unstable arc may cause it to intersect a nonadjacent arc. This forms a closed loops that traps the invaded fluid. Arcs stop at the system boundary. Growth is continued until a stable interface is found. The pressure is then increased until the invading fluid percolates. Small increments in p are used to simulate quasistatic motion. The sequence of p 's affects the fraction of trapped fluid, but changes in \bar{w} are negligible. For a uniform system ($r_1=r_2$) a regular faceted pattern with the lattice symmetry is found in agreement with ex-

periment.¹

This growth algorithm differs in several ways from the IP model.^{2,3} The microscopic configuration of the interface is not calculated in IP. Instead, each throat is assigned a critical p where the arc becomes unstable, which is independent of the configuration of the interface and the direction of invasion. In general this model can only describe bursts. Touches depend on flow direction, and overlap is a cooperative mechanism which depends on both flow direction and the configuration of adjacent arcs. Another difference is that IP growth occurs at the least stable throat at each step. This corresponds to growth at constant infinitesimal flow rather than constant p .

Figure 2 shows the marked change in the invaded pattern as θ decreases from the NW limit. Growth was started from a ring of unit radius around a central disk. For each θ , the ring center was varied to give percolation at the lowest p . Values of p where growth started also varies with θ and the position of the starting ring.

One obvious change with decreasing θ is an increase in

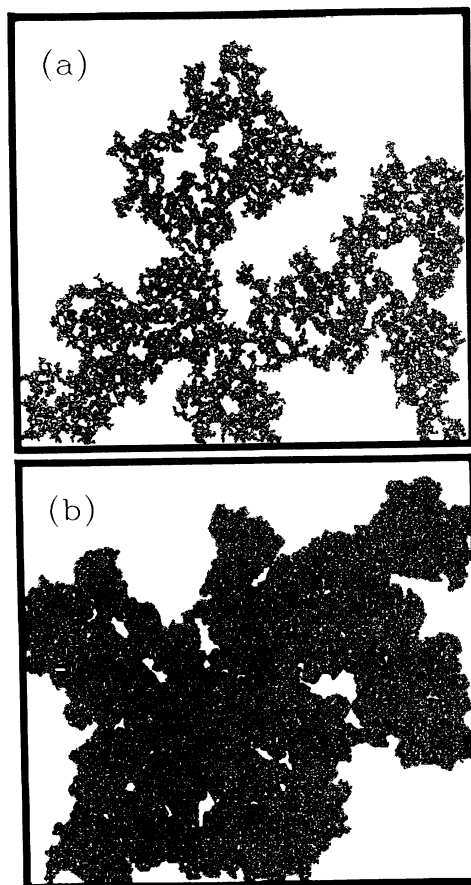


FIG. 2. Percolating patterns for sample A with $L=300$ and (a) $\theta=179^\circ$, and (b) $\theta=58^\circ$. The invading fluid is black, disks and invaded fluid are white.

\bar{w} . Slices through each pattern were made and the distribution of widths of the invaded segments found. The mean width \bar{w} gave the most reproducible measure and is plotted in Fig. 3. Fluctuations with the choice of starting ring, sequence of p 's, and stage of growth were of order 5%. The second moment of the distribution and exponential decay rate at large w showed similar scaling with θ , as did measures based on surface normal correlations and bulk and interface density correlations.

Figure 3 shows the growth of \bar{w} as θ decreases for the systems listed in Table I. For all cases \bar{w} appears to diverge at a critical angle θ_c which decreases with the porosity ϕ , i.e., the area fraction of the pore space (Table I). Dotted lines in Fig. 3 are power-law fits, $\bar{w}(\theta) - \bar{w}(180^\circ) \propto (\theta - \theta_c)^{-\nu}$ with $\nu \approx 2.3$ and θ_c from Table I. Because of finite sample size, uncertainties are of order ± 0.5 in ν and $+3^\circ$ or -5° in θ_c .

Below θ_c a stable percolating interface could not be produced for any sequence of pressures or starting ring. Once p was large enough to initiate growth across the sample, flow continued in a uniform flood which filled the system. In general the pressure to initiate flow decreased as the radius of the starting ring increased. This was also seen just above θ_c where starting rings of radius ≈ 10 were needed to produce stable percolating interfaces. The variation of p with radius is reminiscent of the effect of a macroscopic surface tension, but fluctuations were too large to establish whether the excess pressure for flow scaled inversely with ring radius.

The divergence of \bar{w} at θ_c results from a change in the dominant growth mechanism. For large θ , \bar{w} has a value near 5 and growth is almost entirely by bursts. The pattern is nearly θ independent, since the hierarchy of pressures where each throat bursts is unchanged. For the same reason, growth from any ring on the pattern in Fig. 2(a) with any sequence of intermediate p 's produces an almost identical pattern. Only the structure of the trapped regions is modified slightly. Furthermore, when the random numbers were chosen so that the hierarchy of throat widths in systems A, B, and C was the same,

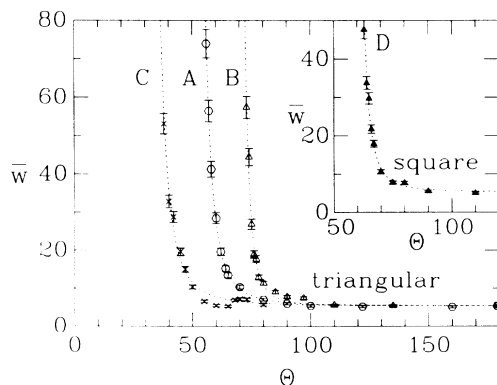


FIG. 3. Divergence of \bar{w} as θ decreases. Error bars are indicated and dotted lines represent power-law fits.

2044

the NW growth patterns were identical.

The predominance of bursts in the NW limit allowed a direct comparison to the IP model. Our algorithm was modified to advance the throat with the lowest bursting pressure at each step. For every p , the outer portion of the stable interface was identical to that obtained with our usual rules. The trapped regions in IP were similar, but somewhat larger. Trapped regions are also the only difference between IP and regular percolation clusters which are known¹⁰ to have similar fractal dimensions d_f . Our results for the triangular lattice are consistent with $d_f \approx 1.9$ at length scales above \bar{w} which is consistent with the value¹⁰ for IP: $d_f = 1.88$. Our statistics were not large enough to fix d_f more precisely or determine whether it varies with θ .

As $\theta \rightarrow \theta_c$, overlaps gain in importance. The pressure for overlap is smallest when the interface makes the most acute angle. In Fig. 1 the interface angle is $\alpha = 120^\circ$ and overlap occurs before bursts for $\theta < 90^\circ$. For the same radii, crossover from bursts to overlap occurs at $\theta \approx 160^\circ$ and 60° for $\alpha = 60^\circ$ and 180° , respectively. For different radii the corresponding crossover angles vary. As θ decreases, overlaps remove less and less acute angles from the interface at pressures where growth can be initiated by bursts. This smoothing continues until θ_c where even $\alpha = 180^\circ$ becomes unstable for most local geometries. Since the crossover angles decrease with ϕ , so does θ_c .

When overlaps and touches are important the pattern is not reproducible. Starting from different points in the cluster for 58° in Fig. 2(b), or using a different sequence of pressures, may produce an entirely different pattern (but a similar \bar{w}). Indeed, the pressure where growth starts for a ring on the cluster may be far above the percolating pressure for many starting rings and may vary with radius.

An interesting variation in the progression of patterns was observed for the most dense system, C. For a narrow range of $\theta (55^\circ - 65^\circ)$ about 95% of growth is by touches. A corresponding peak in \bar{w} appears in Fig. 3. Touches should continue to increase in importance as ϕ decreases. Since they do not reflect cooperation by neighboring arcs, they should not lead to a divergence in \bar{w} . By superseding overlaps they may actually depress θ_c or even remove the transition.

Related studies of growth mechanisms in square tube networks have been presented by Lenormand and co-workers.^{2,6} They find that bursts dominate NW invasion leading to IP patterns. Mechanisms corresponding to overlap of three arcs and overlap of two arcs followed by a touch dominate the W limit and lead to a smoother interface. While intermediate θ 's have not been studied, one may expect a dynamical transition similar to that found here.

In conclusion, we have presented evidence of a dynamical phase transition associated with changes in local growth modes in a model porous medium. Below a critical contact angle θ_c , fluid advances in a stable flood.

Above θ_c the fluid percolates at constant pressure. The width of fingers in the percolating pattern diverges as $\theta \rightarrow \theta_c$. This transition appears to be independent of the exact pore geometry, but θ_c varies with porosity.

We have studied this transition in the lowest number of dimensions where it can be defined. The interface is 1D and will be roughened by arbitrarily weak disorder. Thus below θ_c an advancing interface is still not smooth. However, we may expect self-affine roughness here rather than fractal structure. By analogy with equilibrium critical phenomena, we expect the transition to occur in more dimensions. Indeed, the greater connectivity of interfaces in 3D should facilitate divergence of the finger width, and lead to smoother advancing fronts below θ_c .

Experiments in the NW and W limits show a marked change in growth patterns which is consistent with our results. However, measurements over a range of contact angles are needed to establish the existence of a transition.

We thank J. R. Banavar, E. Herbolzheimer, P. Meakin, J. P. Stokes, and D. A. Weitz for useful discussions, and SUN Microsystems for donated work stations used in this study. Support from the National Science Foundation through Grant NO. DMR-8553271 and matching funds from the Exxon Education Foundation is gratefully acknowledged. One of us (M.O.R.) also acknowledges support from the Sloan Foundation.

^(a)On leave from Institute of Theoretical Physics, 00-681 Warsaw, Poland.

¹E. Ben-Jacob, R. Godbey, N. D. Goldenfeld, J. Koplik, H. Levine, T. Mueller, and L. M. Sander, Phys. Rev. Lett. **55**, 1315 (1985).

²R. Lenormand and C. Zarccone, Phys. Rev. Lett. **54**, 2226 (1985); R. Lenormand, C. Zarccone, and A. Zorr, J. Fluid Mech. **135**, 337 (1983).

³R. Lenormand, C. R. Seances Acad. Sci. Ser. B **291**, 279 (1980); R. Chandler, J. Koplik, K. Lerman, and J. F. Willemssen, J. Fluid Mech. **119**, 249 (1982).

⁴L. Patterson, Phys. Rev. Lett. **52**, 1621 (1984).

⁵K. Maloy, J. Feder, and T. Jossang, Phys. Rev. Lett. **55**, 2688 (1985).

⁶R. Lenormand and C. Zarccone, in *Proceedings of the Fifty-Ninth Annual Technological Conference and Exhibition of the Society of Petroleum Engineers, Houston, Texas, 16-19 September 1984* (Society of Petroleum Engineers, Richardson, TX, 1984); R. Lenormand, C. Zarccone, and E. Touboul, J. Fluid Mech. **187**, 165 (1988).

⁷J. P. Stokes, D. A. Weitz, J. P. Gollub, A. Dougherty, M. O. Robbins, P. M. Chaikin, and H. M. Lindsay, Phys. Rev. Lett. **57**, 1718 (1986).

⁸A fluid interface intersects a solid at a θ fixed by the balance of surface energies; see P. G. de Gennes, Rev. Mod. Phys. **57**, 827 (1985).

⁹W. G. Anderson, JPT J. Pet. Technol. **39**, 1453 (1987).

¹⁰D. Wilkinson and J. F. Willemssen, J. Phys. A **16**, 3365 (1983).

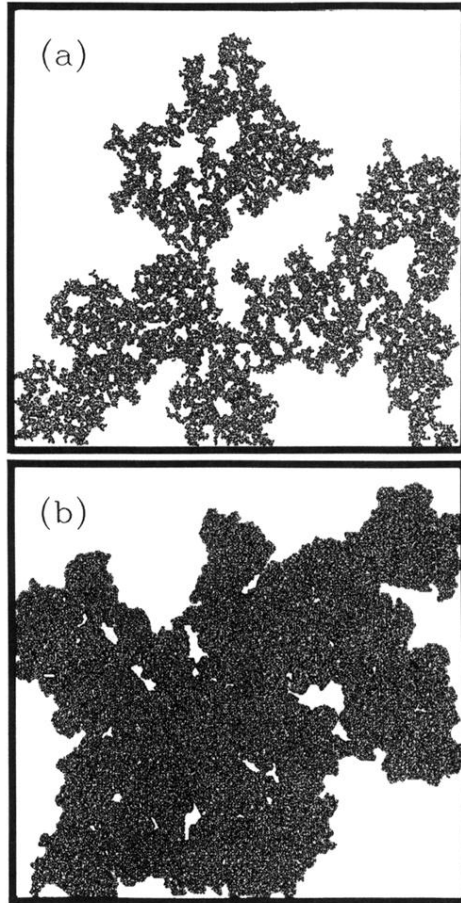


FIG. 2. Percolating patterns for sample A with $L = 300$ and (a) $\theta = 179^\circ$, and (b) $\theta = 58^\circ$. The invading fluid is black, disks and invaded fluid are white.